Biomedicine & Pharmacotherapy 139 (2021) 111648

Contents lists available at ScienceDirect

Biomedicine & Pharmacotherapy

journal homepage: www.elsevier.com/locate/biopha

Original article

Rutaecarpine administration inhibits cancer cell growth in allogenic TRAMP-C1 prostate cancer mice correlating with immune balance *in vivo*

Jin-Yuarn Lin *, Tzu-He Yeh

Department of Food Science and Biotechnology, National Chung Hsing University, 250 Kuokuang Road, Taichung 40227, Taiwan

ARTICLE INFO

Keywords:
Allogenic TRAMP-C1 prostate cancer C57BL/6J mice
Cancer immunotherapy
M1/M2 cytokines
Rutaecarpine
Th1/Th2 cytokines

ABSTRACT

Background: Rutaecarpine (Rut) is a plant alkaloid abundant in *Euodia ruticarpa* which is a Chinese herbal medicine used for treating various cancers. However, the Rut administration effect on prostate cancer in vivo remains unclear.

Aim: In the present study we established an allogenic TRAMP-C1 prostate cancer mouse model to evaluate the Rut administration effect and mechanism in vivo.

Methods: To unravel the Rut administration effect on prostate cancer in vivo, C57BL/6J male mice (8 weeks old) were randomly grouped ($n = 9$), subcutaneously loaded with TRAMP-C1 prostate cancer cells and immediately given daily by gavage with Rut dissolved in soybean oil at 7 mg (low dose), 35 mg (medium dose), and 70 mg/kg b.w./day (high dose) for successive 39 days.

Results: Rut administration significantly and dose-dependently reduced both tumor volume and solid prostate cancer weight in allogenic TRAMP-C1 male mice. Rut administration markedly increased (TNF-α+IFN-γ) (Th1-)/IL-10 (Th2-) cytokine secretion ratios by splenocytes and TNF-α (M1-)/IL-10 (M2-) cytokine secretion ratios by macrophages as compared to those of dietary control group, suggesting that Rut administration in vivo regulates the immune balance toward Th1- and M1-polarized characteristics. Decreased $CD19^+$, $CD4^+$ and $CD8^+$ lymphocytes in the peripheral blood of allogenic TRAMP-C1 mice were significantly elevated by Rut administration. Tumor weights positively correlated with TNF-α secretions by splenocytes, suggesting that there is a tumor cachexia in the tumor-bearing mice. Tumor weights negatively correlated with IgG (Th1-antibody) levels in the sera, suggesting that Th1-polarized immune balance may inhibit prostate cancer cell growth.

Conclusions: Our results evidenced that Rut administration suppresses prostate cancer cell growth in mice subcutaneously loaded with TRAMP-C1 cells and correlated the anti-cancer effects with Th1-polarized immune balance in vivo.

1. Introduction

Statistics for cancers by American Cancer Society indicate that prostate cancer is the leading cause of cancer death in males [1]. Prostate cancer, one of malignant tumors, is a disease of abnormal cell growth due to uncontrolled cell division and subsequently causes tumor formation. Some tumors have the ability to invade adjacent parts of the body or metastasize to other organs. Distant metastasis is the main cause of death in cancer patients [2,3]. During cancer development chronic inflammation is the beginning disease stage [4]. There are a variety of leukocyte populations involving in this chronic inflammation, such as macrophages, neutrophils, eosinophils, and mast cells. Macrophages, play an important role in enhancing the invasion, metastasis of cancer cells, and the development of cancer-related inflammation (CRI) [5,6]. Therefore, the control of excess CRI in the tumor microenvironment may be an effective strategy to prevent the invasion and metastasis of cancer cells. Traditional methods of treating cancers involve discovering and eliminating cancer cells through surgery, radiotherapy, or

Abbreviation: AR-V7, androgen receptor splice variant 7; CD, cluster of differentiation; Con A, concanavalin A; CRPC, castration-resistant prostate cancer; ER, *Euodia ruticarpa*; GRP78, glucose-regulated protein 78; IFN, interferon; Ig, immunoglobulin; IL, interleukin; JNK, c-Jun N-terminal kinase; LPS, lipopolysaccharide; M1, type 1 macrophage; M2, type 2 macrophage; PERK, PKR-endoplasmic reticulum (ER)-related kinase; Rut, rutaecarpine; SIAH2, seven in absentia homolog 2 (Drosophila); TCM, traditional Chinese medicine; Th1, type 1 helper T cell; Th2, type 2 helper T cell; TNF, tumor necrosis factor.

* Corresponding author.
E-mail address: jinlin@nchu.edu.tw (J.-Y. Lin).

https://doi.org/10.1016/j.biopha.2021.111648
Received 3 March 2021; Received in revised form 12 April 2021; Accepted 19 April 2021
Available online 1 May 2021

chemotherapy. However, tumor prevention and control through active components isolated from health foods and traditional herbal medicines have gradually become auxiliary treatments. Looking for anti-tumor drugs targeted at immunotherapy from different materials with low toxicity has become the cancer prevention and control research focus [7].

Macrophages in the tumor microenvironment are generally classified into two types, including classically activated macrophages (type 1, M1-type) and alternatively activated macrophages (type 2, M2-tpye) [8,9]. In general, M1-type macrophages increase the secretion of pro-inflammatory cytokines, including IFN-γ, TNF-α, IL-6, and IL-1β, that tend to promote type 1 helper T cells (Th1) immune responses in inhibiting cell proliferation and tissue destruction, and anti-tumor drug resistance [10]. In contrast, M2-type macrophages potentially secrete an anti-inflammatory cytokine IL-10 after they are stimulated by Th2 cytokines, such as IL-4 or IL-13, and inhibit TNF-α and IL-6 secretions; in general, M2 cells may have the anti-inflammatory ability, but they are advantageous to cancer cells proliferation and tissue repair [11]. Helper T cells (Th) are highly related to macrophages differentiation and functions. Th1 cells activate M1 macrophages to secrete IFN-γ, which are considered to be pro-inflammatory. In contrast, Th2 cells produce IL-4, IL-5, and IL-10 that can inhibit Th1 cells' secretion to achieve an anti-inflammatory state [12]. Moreover, the M1 and M2 macrophage classification is based on the Th1/Th2 dichotomy. The polarization for the M1 type macrophages may promote the Th1 immune balance and M2 type macrophages enhance Th2 immune responses [13]. Although the development of cancer to date is still in chaos, the differentiated ratios of M1/M2 and Th1/Th2 cells in the tumor microenvironment are undoubtedly of importance to control the cancer development progress. In advance, the immune system itself including NK cells and cytotoxic T cells can detect and kill cancer cells, further suggesting that $CD8^+$ cytotoxic T lymphocytes with anti-cancer activity is a prerequisite for immunotherapy [14,15].

Recently, it was found that active components extracted from health foods and traditional herb medicines may regulate Th1/Th2 and/or M1/M2 cells differentiation and may be further applied to treat or prevent cancer development using indirect immunotherapy [16–18]. *Euodia ruticarpa* (ER) (also known as Wu Zhu Yu) is one of traditional medicinal herbs in Taiwan that is mainly used for the treatment of headaches, diarrhea, amenorrhea, and hypertension [19–21]. The main chemical constituents of ER include alkaloids, terpenoids, phenols and volatile oils [21,22]. Among alkaloids, rutaecarpine (Rut) is an active component isolated from immature ER fruits with pharmacological activities, including anti-hypoxia, alleviating migraine, anti-inflammatory, anti--hypertensive, and anti-angiogenesis effects [23–29]. Most herbs used for Traditional Chinese medicine (TCM) are rich in alkaloids such as Rut in ER and have preventive or anti-cancer effects [30–32]. TCM or its active components that are characterized by multiple pathways and targets can play many important roles in treating symptoms and root causes of diseases, such as inhibiting or killing tumor cells, and promoting the immunity in cancer patients after surgery.

Rut is an active alkaloid in ER with different pharmacological activities. There are some in vitro and cell-based studies evidencing the correlation of Rut treatment and prostate cancer. Recently, Rut has been used for treating castration-resistant prostate cancer (CRPC) and found to inhibit cell growth of CRPC through inducing the formation of the GRP78-AR-V7-SIAH2 degradation complex and cell cycle arrest in the G0/G1 phase in vitro [33]. Moreover, Rut administration inhibits the tumor size and weight in the 22Rv1 (a human prostate carcinoma epithelial cell line) xenograft animal model, reduces the protein levels of Ki67 and AR-V7 in the xenograft tissue, synergistically enhances the sensitivity of CRPC to antiandrogen agents (e.g., enza and bicalutamide), and suppresses the proliferation of CRPC in vivo [33]. However, the Rut administration effect on prostate cancer in vivo remains unclear. To evaluate the Rut administration effect on prostate cancer, TRAMP-C1 prostate cancer cells were subcutaneously loaded in C57BL/6J male mice for 39 days to clarify the underlying mechanisms.

2. Materials and methods

2.1. Sample

Rutaecarpine (CAS RN: 84–26-4; $C_{18}H_{13}N_3O$; MW, 287.32) was purchased at its highest purity (>98%, HPLC reagent grade) from Tokyo Chemical Industry Co., Ltd., Japan.

2.2. Experimental animals and grouping

C57BL/6J male mice (6 weeks old) were purchased from the National Laboratory Animal Center, National Applied Research Laboratories, National Science Council in Taipei, ROC and maintained in the Department of Food Science and Biotechnology at National Chung Hsing University in Taichung, Taiwan, ROC. The animal room environmental condition was kept on a 12 h-light/12 h-dark cycle, constant temperature at 23 ± 2 ºC and ambient humidity at 50–75%. The mice were kept on a chow diet (laboratory standard diet, Diet MF 18, Oriental Yeast Co., Ltd., Osaka, Japan) to acclimatize for 2 weeks. After acclimation, the C57BL/6J mice (8 weeks old) were randomly divided into seven groups ($n = 9$) at day −1, including non-treatment control (NTC, normal mice without any treatment), vehicle control (VC, only matrigel without cancer cells), positive control (PC, intraperitoneal injection (i.p.) weekly with 0.1 mL of 1 mg/mL paclitaxel (Sigma, T-7402, St. Louis, Missouri, USA) dissolved in sterile saline (0.85% NaCl), DC (Dietary control, 0.2 mL soybean oil/mouse/day), low dose of Rut (RL, 7 mg/kg b.w./day by gavage), medium dose of Rut (RM, 35 mg/kg b.w./day by gavage) and high dose of Rut (RH, 70 mg/kg b.w./day by gavage). There were no significant differences among groups in initial average body weight. After grouping, experimental feed was provided with AIN-76 feed according to the American Institute of Nutrition recommendation to satisfy the nutritional requirement of all experiment mice [34]. Each 1000 g AIN-76 feed was composed of 400 g sucrose, 250 g corn starch, 200 g casein, 50 g fiber, 35 g mineral mixture, 10 g vitamin mixture, 3 g DL-methionine, 2 g choline bitartrate and 50 g soybean oil. Mice in all groups were provided with enough water and food ad libitum. To evaluate the Rut administration effect, Rut was dissolved in soybean oil daily and provided with an aliquot of 0.2 mL/day by gavage from day 0. VC, PC and DC groups were fed 0.2 mL soybean oil daily by gavage during the 39-days experiment period. During the experiment period, mouse food intake and body weight change were taken down twice a week. The used doses of Rut were calculated based on our preliminary in vitro cell experiments. We found that Rut treatment at 25 μM (= 25 μmol/1000 mL = 0.025 μmol/mL = 0.025 × 287.3 g/mol × 10^{-6} mol/mL = 7.1825 μg/mL = 0.007 mg/mL) is an effective concentration without cytotoxicity to splenocytes at the cell density of 5 × 10^6 cells/mL in vitro. The ratio of 25 μM Rut versus 5 × 10^6 cells/mL (namely, 0.007 mg Rut versus 5 × 10^6 cells) was selected as the lowest dose used in vivo. However, total splenocytes in a spleen of a 20 g mouse were about 1 × 10^8 cells which are 20 folds of 5 × 10^6 cells. Therefore, an aliquot of 0.14 mg (0.007 mg × 20 = 0.14 mg) Rut was selected as a low dose (RL group, 1×) to furnish a 20 g mouse daily (0.14 mg Rut/20 g mouse/day = 7 mg/kg b.w./day). The doses of 35 mg/kg b.w./day and 70 mg/kg b.w./day were selected as medium (RM group, 5×) and high dose Rut (RH group, 10×), respectively. The experiment mice did not die due to subcutaneously loaded with TRAMP-C1 cells or Rut administration during the experiment period. The animal use and experimental protocol for this study was examined and approved (IACUC No: 103-119) by the Institutional Animal Care and Use Committee of National Chung Hsing University, Taichung, Taiwan.

2.3. Culture and harvest of prostate cancer TRAMP-C1 cells

TRAMP-C1 cells (ATCC CRL-2730, from transgenic mouse prostate

adenocarcinoma), was kindly gifted from Dr. Chi-Shiun Chiang-Department of Biomedical Engineering and Environmental Sciences, National Tsing Hua University, Hsin Chu, Taiwan. Cells were maintained in Dulbecco's Modified Eagle's Medium (DMEM) supplemented with 10% (v/v) fetal bovine serum (FBS, GIBCO, Grand Island, NY, USA), 5 μg/mL insulin (Roche, Indianapolis, IN, USA), 10^{-8} M 5α-dihydrotestosterone (DHT, Sigma, St. Louis, MO, USA) and PSA antibiotics including penicillin 100 units/mL, streptomycin 100 μg/mL, and amphotericin B 0.25 μg/mL and cultured in a humidified incubator at 37 °C with 5% CO_2 and 95% air. The cultured cells were sub-cultured when they achieved 90% confluence in the culture plate. Cells at passages 4–10 were harvested to perform the following experiment.

2.4. Ectopic mouse tumor models

To establish an ectopic tumor implantation model in allogeneic tumor animals, the harvested TRAMP-C1 viable cells were counted and adjusted to an appropriate cell density using the trypan blue dye exclusion assay. Aliquots of 5×10^4 cells were suspended in 0.1 mL matrigel (Matrigel® Basement Membrane Matrix, Corning, NY, USA). The final concentration was 5 mg/mL suspended in phosphate-buffered saline (PBS, containing 8.1 mM Na_2HPO_4, 1.5 mM KH_2PO_4, 137 mM NaCl and 2.7 mM KCl, pH 7.4, 0.2 μm filtered). Each individual mouse in all groups except NTC and VC groups received 5×10^4 cells with 0.1 mL matrigel by subcutaneous injection into the lower right groin to create a solid tumor animal model at day 0 of the experiment interval. The VC group received only 0.1 mL matrigel without cancer cells. Tumor growth in the experimental mice was observed on a daily basis. Mice body weight and tumor size in each group were recorded twice a week. The extent of orthotopic tumor size was measured twice a week. The mouse was sacrificed humanely when the tumor was larger than 20 mm. All experimental mice survived during the experimental period. At the end of the experiment (39 days of post-injection), the mice were sacrificed humanely to collect and analyze the immune cells, organs, plasma, and tumors. The experimental mice organs including the thymus, heart, lung, liver, spleen, kidney, testis and epididymal fat were weighed and expressed as absolute tissue weight (ATW) and relative tissue weight (RTW); RTW = [mouse organ weight (g)/mouse body weight (g)] ×100. After the mouse was sacrificed, the tumor was stripped, weighed and tumor volume measured. The tumor volume was calculated and expressed by the following equation; tumor volume (cm^3) = length (cm) × width (cm) × height (cm)/2. Finally, tumor inhibition rate by Rut administration was calculated according to the following formula; tumor inhibition rate (%) = [1 – (tumor weight of the sample treated mouse/mean tumor weight of dietary control group)] × 100.

2.5. Determination of blood $CD3^+$, $CD4^+$, $CD8^+$, and $CD19^+$ cells in the allogeneic TRAMP-C1 prostate cancer mice using flow cytometry

At the end of the experiment (at day 38), 100 μL whole blood of the experiment mice was drew out using retro-orbital venous plexus puncture under 2% vapor isoflurane anesthesia. $CD3^+$ (Total T cells), $CD4^+$ (helper T cells), $CD8^+$ (cytotoxic T lymphocyte), and $CD19^+$ (total B cells) cells in the peripheral blood were detected by specific antibodies and measured using flow cytometry, respectively. Briefly, an aliquot of 50 μL of whole blood from each individual mouse was stained with 1 μg anti-mouse $CD3^+$ PE, and 1 μg anti-$CD19^+$ FITC antibody (BD Falcon, NJ, USA), and another 50 μL whole blood was stained with 1 μg anti-CD8a PE, and 1 μg anti-$CD4^+$ FITC antibody (BD Falcon, NJ, USA) in the flow tube for 15 min in the dark, respectively. The reactant mixture was then incubated with lysing solution for fluorescence activated cell sorting (FACS) to lyse for 10 min. The flow tube was centrifuged at 25 °C, 300g for 5 min. The flow tube was washed twice with 0.5 mL staining buffer. Finally, the percentages of $CD3^+$ and $CD19^+$, as well as $CD4^+$ and $CD8^+$ were respectively determined by flow cytometry (Beckman Coulter, FC500, California, USA).

2.6. Rut administration effects on serum titers of non-specific antibodies in the allogeneic TRAMP-C1 prostate cancer mice

At the end of the experiment (at day 39), 2% isoflurane (cat. no., 4900–1605, Panion & BF Biotech Inc., Taipei, Taiwan) was used to anesthetize the mice with a vaporizer (CAS-01, Northern Vaporizer Limited, Cheshire, England, UK). The blood was taken using retro-orbital venous plexus puncture and collected into a micro centrifuge tube. Immediately after the blood was collected, the experimental mice were sacrificed with CO_2 inhalation [28]. Peritoneal macrophages and splenocytes of the experiment mice were isolated aseptically. The experimental mice organs were removed and weighed. Each collected whole blood was stood at room temperature for 2 h to agglutinate the blood cells. The micro centrifuge tube was centrifuged at 12000g for 20 min. The serum was collected into another micro centrifuge tube and stored at −80 °C for non-specific antibodies analyses. The levels of non-specific antibodies were respectively detected using mouse IgA, IgE, IgG, and IgM enzyme linked immunosorbent assay (ELISA) kits (mouse Ig ELISA quantitation kits, Bethyl Laboratories, Inc., TX, USA) and performed according to the manufacturer's protocol. The ELISA kit detection limit (LOD) used in this study was <3.9 pg/mL.

2.7. Isolation of primary immune cells from the allogeneic TRAMP-C1 prostate cancer mice

At the end of the experiment (at day 39), the experimental mice were sacrificed humanely to isolate primary immune cells including splenocytes and peritoneal macrophages. The isolation procedure was performed as described previously [35]. After primary immune cells including splenocytes and peritoneal macrophages were isolated, the viable cells were counted and adjusted by trypan blue exclusion method with a hemocytometer. The isolated splenocytes and macrophages were respectively adjusted to a cell density of to 1×10^7 cells/mL and 2×10^6 cells/mL for use.

2.8. Rut administration effects on Th1 (TNF-α and IFN-γ)/Th2 (IL-10) cytokines secreted levels by primary splenocytes in the allogenic TRAMP-C1 prostate cancer mice

To assess the Rut administration effects on Th1/Th2 immune balance in the allogeneic TRAMP-C1 prostate cancer mice, isolated splenocytes (1×10^7 cells/mL, 500 μL/well) from the mice of different groups were cultured with 500 μL/well TCM medium, lipopolysaccharide (LPS, a B-cell mitogen, Sigma-Aldrich Co., L-2654, St. Louis, MO, USA) or concanavalin A (ConA, a T-cell mitogen, Sigma-Aldrich Co., C2010, Schnelldorf, Germany) at the final concentration of 2.5 μg/mL in a 24-well plate. The plate was incubated in a humidified incubator with 5% CO_2 and 95% air at 37 ℃ for 48 h. After incubation, the plate was centrifuged at 400g for 10 min, the supernatant was collected and stored at −80 °C for the following Th1/Th2 cytokine assays. Levels of Th1 [tumor necrosis factor (TNF)-α and interferon-γ (IFN-γ)] and Th2 [interleukin (IL)−10] cytokines were measured by enzyme linked immunosorbent assay (ELISA) using ELISA kits (mouse DuoSet ELISA Development system, R&D Systems, MN, USA) and performed according to the manufacturer's instruction. The limit of detection (LOD) of the ELISA kits used in this study was <15.6 pg/mL.

2.9. Rut administration effects on M1 (pro-)/M2 (anti-inflammatory) cytokines secreted by mouse peritoneal macrophages in the allogenic TRAMP-C1 prostate cancer mice

To assess the Rut administration effects on M1 (pro-)/M2 (anti-inflammatory) cytokines secreted by peritoneal macrophages in the allogeneic prostate cancer mice, mouse primary peritoneal macrophages (2×10^6 cells/mL, 500 μL/well) in the absence or presence of LPS (an endotoxin) at a final concentration of 2.5 μg/mL were incubated in a

humidified incubator with 5% CO_2 and 95% air at 37 °C for 48 h. After incubation, the cell culture supernatant was collected and stored at −80 °C for M1/M2 cytokines assay using ELISA kits (mouse DuoSet ELISA Development system, R&D Systems, MN, USA) and performed according to the manufacturer's protocol. The Elisa kit detection limit (LOD) used in this study was <15.6 pg/mL.

2.10. Data analysis

Results are presented as the mean ± standard error of mean (SEM). The statistical significance of data was analyzed using one-way ANOVA followed by Duncan test and Dunnett's post hoc test. Relationships between different parameters were analyzed using the Pearson product-moment correlation coefficient (r). The p value lower than 0.05 was considered significant.

3. Results

3.1. Rut administration effect on body weights and visceral weights in allogeneic TRAMP-C1 prostate cancer mice

In the present study a prostate cancer mouse model subcutaneously loaded with TRAMP-C1 cells was established to evaluate the Rut administration effects against prostate tumorigenesis. Different Rut doses were administered by gavage for successive 39 days. In the positive control (PC) group C57BL/6 J mice were intraperitoneally injected (i.p.) with paclitaxel (1 mg/mL, 0.1 mL) weekly from day 0. The results showed that initial body weights of C57BL/6 J mice was not significantly different ($p > 0.05$) among the groups, and body weights of experimental mice in all the groups gradually increased during the experiment period (Fig. S1(A)). However, both dietary control (DC) and PC groups have significantly ($p < 0.05$) higher body weights than those of the other groups at the end of the experiment (Fig. S1(A) and Table S1). Contrary to our prediction, the body weights of Rut-fed groups were significantly ($p < 0.05$) lower than those of DC and PC groups at the end of the experiment (Fig. S1(A) and Table S1). To clarify the puzzle, the tumor weight was deducted from the body weight of corresponding experiment mice to obtain individual net body weight. The results exhibited that the net body weight of Rut-fed groups significantly but not obviously decreased compared to that of the DC group (Fig. S1(B)). However, the net body weight of all experiment groups was close to that of the vehicle control (VC) group. To further clarify the Rut administration effect on the experiment mice, feed intake and visceral weights of the experiment mice were measured (Table S1 and Table S2). No considerable differences were observed in feed and energy intakes, feed efficiencies, as well as visceral weights in Rut-fed groups as compared to those of the DC group. The observation indicated that tube feeding with Rut at different doses did not significantly influence feed intakes and visceral weights, suggesting that Rut administration by gavage at the doses used in this study have little toxicity to the experiment mice.

3.2. Rut administration effect on tumor volume, tumor weight, and tumor inhibition rate in allogeneic TRAMP-C1 prostate cancer mice

During the experiment interval, tumor volumes in the experimental mice were measured (Fig. 1). We observed that subcutaneous tumors in the experiment mice gradually bulged up at the 18 days. At the 22 days, the size of the subcutaneous tumor in the DC group was significantly larger than that in the other groups ($p < 0.05$). In contrast to the DC group (given soy oil only), the tumor diameter in the RH group was much smaller than that in the DC group. We found that tube feeding with Rut at the high dose (RH group) and treatment with paclitaxel i.p. (PC group) at the end of the experiment significantly ($p < 0.05$) reduced tumor volumes as compared to that of experiment mice in the DC group although the tumor volumes gradually increased during the experiment

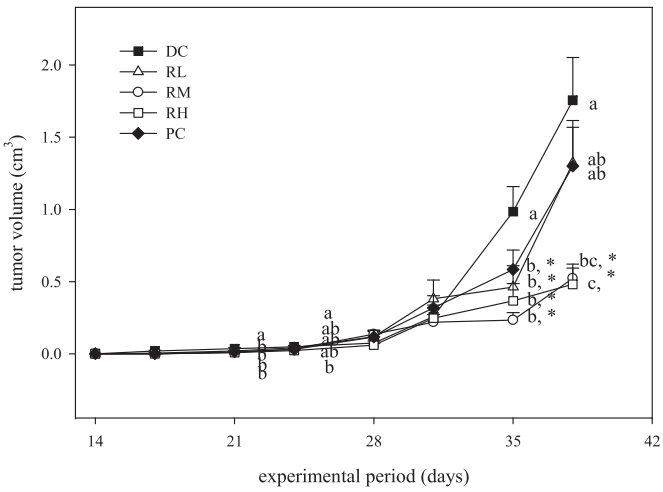

Fig. 1. Rutaecarpine administration effects with different doses on changes in tumor volume in male C57BL/6J mice subcutaneously loaded with TRAMP-C1 cells during the 39-days experiment period. Values are means ± SEM ($n = 7–9$). Each point at same experimental period among groups not sharing a common small letter (a, b, c) are significantly different ($p < 0.05$) from each other analyzed by one-way ANOVA, followed by Duncan's multiple range test. *, Significant differences from DC group analyzed with one-way ANOVA, followed by Dunnett's post hoc test. NTC, non-treatment control; VC, vehicle control; DC, dietary control; RL, low dose rutaecarpine; RM, medium dose rutaecarpine; RH, high dose rutaecarpine; PC, paclitaxel treatment i.p., a positive control.

period. At the end of the experiment, TRAMP-C1 prostate cancers in the experiment mice were removed, and the tumor volume and tumor weight were measured (Fig. 2). The tumor appearance (Fig. 2(A)), tumor volume (Fig. 2(B)) and tumor weight (Fig. 2(C)) evidenced that Rut administration (particularly RH group) and paclitaxel treatment i.p. (PC group) significantly inhibited TRAMP-C1 prostate cancer growth in vivo compared to those of the DC group. Most importantly, Rat administration significantly ($p < 0.05$) inhibited the tumor weights and increased the tumor inhibition rate dose-dependently (Table 1). The tumor inhibition rate in the RH group achieved 56.0% (Table 1), suggesting that Rut administration has a markedly inhibitory effect on TRAMP-C1 solid tumor growth in the experiment mice. Importantly, the inhibitory effect of Rut administration at the higher doses (RM and RH groups) was much better than paclitaxel i.p. treatment, suggesting that Rut administration may be realistically applied to treat prostate cancer in vivo.

3.3. Rut administration effects on Th1/Th2 cytokines secretion by splenocytes isolated from allogeneic TRAMP-C1 prostate cancer mice

To evaluate the Th1/Th2 immune balance changes in TRAMP-C1 tumor-bearing mice influenced by Rut administration, Th1 (TNF-α, IFN-γ) and Th2 (IL-10) secretions by splenocytes from the C57BL/6J male mice subcutaneously loaded mouse prostate cancer TRAMP-C1 cells for 39 days were measured (Fig. 3). The results in Fig. 3 show that both IFN-γ and IL-10 secretions increased dose-dependently in the spontaneous state (without extra stimulation in vitro) in Rut tube-feeding groups compared with those of DC group. This suggests that Rut administration may increase the immunity in the TRAMP-C1 tumor-bearing mice via increasing Th1/Th2 cytokines secretion. Under LPS stimulation, the RH group significantly increased TNF-α and IL-10 secretions compared with the DC group, further indicating that Rut administration may increase immunity in the TRAMP-C1 tumor-bearing mice via increasing Th1/Th2 cytokines secretion. Under Con A stimulation, no significant differences were found in Rut-fed groups compared to the DC group. However, paclitaxel treatment i.p. (PC group) significantly increased (TNF-α + IFN-γ)/IL-10 (Th1/Th2) cytokine secretion ratios by splenocytes, suggesting that paclitaxel i.p. may induce a Th1-

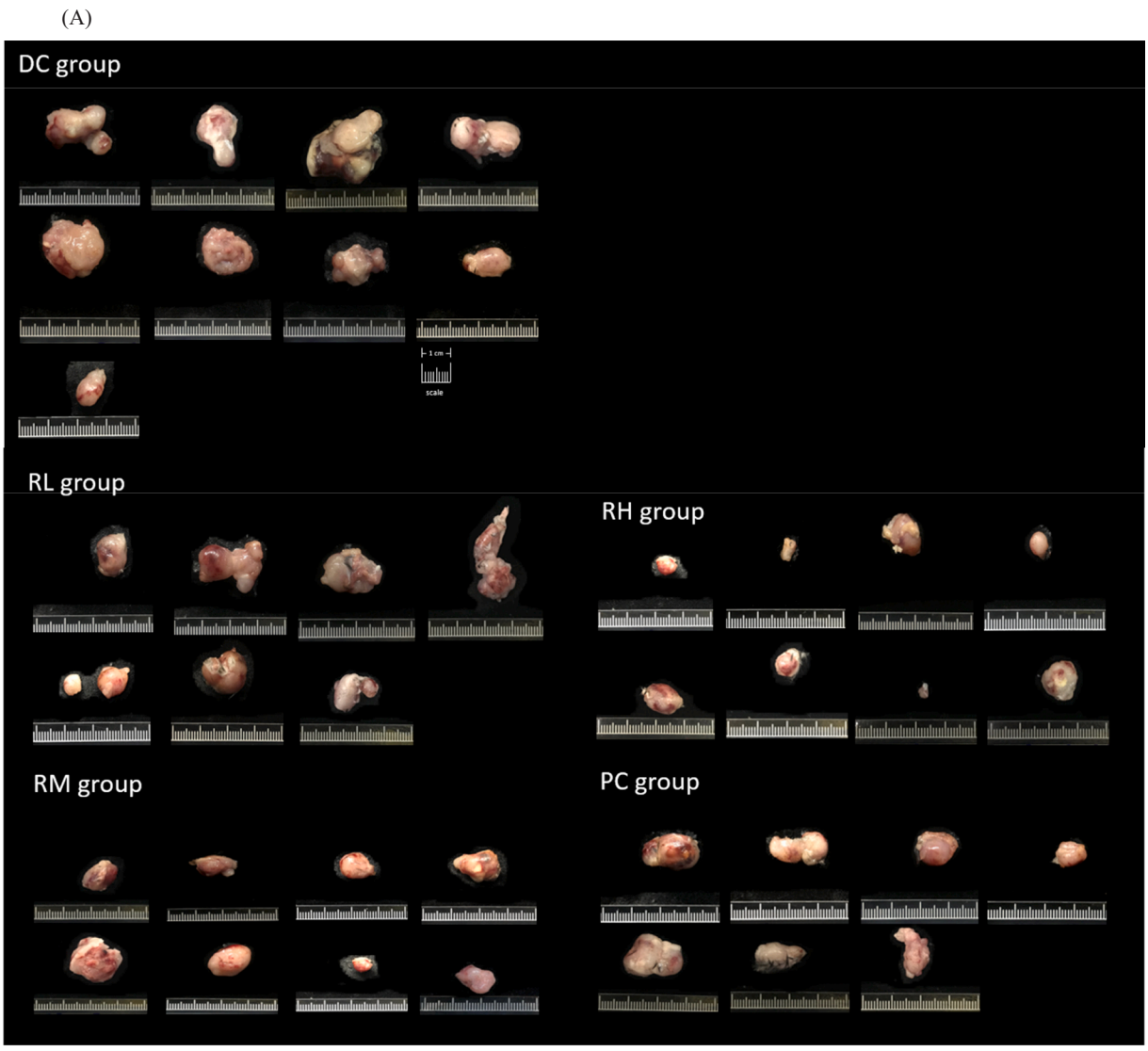

Fig. 2. Rutaecarpine administration effects with different doses on tumor appearances **(A)**, tumor volume **(B)**, and tumor weight **(C)** of male C57BL/6J mice subcutaneously loaded with TRAMP-C1 cells for 39 days. Values are means ± SEM ($n = 7$–9). Bars not sharing a common small letter (a, b, c) are significantly different ($p < 0.05$) from each other analyzed by one-way ANOVA, followed by Duncan's multiple range test. * Significant differences from DC group analyzed with one-way ANOVA, followed by Dunnett's post hoc test. NTC, non-treatment control; VC, vehicle control; DC, dietary control; RL, low dose rutaecarpine; RM, medium dose rutaecarpine; RH, high dose rutaecarpine; PC, paclitaxel treatment i.p., a positive control.

Table 1
Rutaecarpine administration effects with different doses on tumor weights of male C57BL/6 J mice subcutaneously loaded with TRAMP-C1 cells for 39 days.

Group	Dose (mg/kg b.w./day)	Tumor weight (g/mouse)	Tumor inhibition rate (%)
DC	–	1.34 ± 0.20^{a}	0.0 ± 14.7^{b}
RL	7	1.01 ± 0.18^{ab}	24.5 ± 13.6^{ab}
RM	35	0.89 ± 0.13^{ab}	33.8 ± 11.2^{ab}
RH	70	0.59 ± 0.15^{b}	$56.0 \pm 21.2^{a,*}$
PC	-[#]	0.95 ± 0.20^{ab}	28.7 ± 14.8^{ab}

Values are means ± SEM (n = 7–9). Values within same column not sharing a common superscript small letter (a, b) are significantly different ($p < 0.05$) from each other analyzed by one-way ANOVA, followed by Duncan's multiple range test.

[*], Significant differences from DC group analyzed with one-way ANOVA, followed by Dunnett's post hoc test. Tumor inhibition rate (%) =[1 - (tumor weight of each treated mouse/mean tumor weight of DC group)] ×100. DC, dietary control; RL, low dose rutaecarpine; RM, medium dose rutaecarpine; RH, high dose rutaecarpine; PC, paclitaxel treatment i.p., a positive control.

[#], intraperitoneally injected (i.p.) weekly with 0.1 mL of 1 mg/mL paclitaxel dissolved in sterile saline.

polarized immune response. Moreover, Rut administration more or less increased (TNF-α + IFN-γ)/IL-10 cytokine secretion ratios by splenocytes, indicating that Rut administration mildly induces a Th1-polarized immune response in the TRAMP-C1 tumor-bearing mice. Overall, our results suggest that Rut administration enhances immunity and the Th1-inclination immune balance, which may renovate detrimental immune responses in the prostate cancer-bearing mice.

3.4. Rut administration effects on M1/M2 cytokines secretion by peritoneal macrophages isolated from allogeneic TRAMP-C1 prostate cancer mice

To evaluate the changes in M1/M2 immune balance in the TRAMP-C1 tumor-bearing mice influenced by Rut administration, M1 (TNF-α, IL-1β, and IL-6) and M2 (IL-10) secretions by peritoneal macrophages from the C57BL/6J male mice subcutaneously loaded with mouse prostate cancer TRAMP-C1 cells were measured (Fig. 4). The results showed that TRAMP-C1 tumor-bearing mice (DC group) had lower M1 (TNF-α, IL-1β and IL-6), M2 (IL-10) secretions and M1 (TNF-α + IL-1β+IL-6)/M2 (IL-10) secretion ratios by peritoneal macrophages under both spontaneous and LPS-stimulated conditions as compared to those in TRAMP-C1 tumor-free mice (VC group). The results suggest that TRAMP-C1 tumor-bearing mice may suffer immunodeficient disorders and M2-polarized immune balance. Importantly, Rut administration and paclitaxel i.p. (PC group) increased TNF-α, IL-1β, and IL-6 secretions as well as TNF-α/IL-10, IL-6/IL-10, and (TNF-α + IL-1β+IL-6)/IL-10 secretion ratios by peritoneal macrophages, but decreased IL-10 secretion compared to those in the DC group. This indicates that Rut administration by gavage and paclitaxel i.p., respectively, obviously enhances immunity and M1-polarized immune balance in the TRAMP-C1 tumor-bearing mice. Tumor-associated M1 or M2 macrophages account for a large part of the immune cell population in the tumor microenvironment. M1 macrophages may secrete IL-6 cytokine to recruit more white blood cells to the inflammation site and enhance the inflammation reaction in the early stage of tumor development, which may be beneficial to clear the tumor. On the contrary, M2 macrophages secret anti-inflammatory IL-10 cytokine which is related to the repair and growth of malignant tumors. Therefore, IL-6/IL-10 secretion ratios by macrophages can reflect an inflammatory status and a differentiation ratio of M1/M2 macrophages in vitro and in vivo. In the present study, IL-6/IL-10 cytokine secretion ratio by peritoneal macrophages was used to compare inflammatory status and M1/M2 macrophages differentiation ratio in vivo. It is suggested that Rut administration may increase M1 cell population in the tumor microenvironment and exert its anti-tumor effect. We conclude that Rut administration and paclitaxel i.p. can increase the immunity and M1-polarized immune balance which may reverse detrimental immune responses in the prostate cancer-bearing mice. Based on the absolute and relative weights of mouse organs in Table S2, we could not find tumor invasion and metastasis in other organs in this animal model. However, the measurement of chemokine/EMT markers/tumor angiogenesis markers is suggested to clarify possible invasion and metastasis of cancer cells in the future. The effect of Rut administration on tumor metastasis remains to be further studied in the future.

3.5. Rut administration effects on serum non-specific antibody levels in allogeneic TRAMP-C1 prostate cancer mice

To evaluate the Rut administration effect on serum non-specific antibody levels in the TRAMP-C1 tumor-bearing mice, serum IgG (Th1-antibody), IgM, IgA and IgE (Th2-antibody) from the experiment mice were measured (Fig. 5). The results showed that serum nonspecific IgG and IgM levels in TRAMP-C1 tumor-bearing mice were obviously, but not significantly ($p > 0.05$), lower than those in normal mice (VC group), suggesting that the immunity in the TRAMP-C1 tumor-bearing mice may be harmed (Fig. 5 (A) and (D)). Importantly, IgM levels in the RL group slightly increased ($p > 0.05$) compared to that in the DC group, suggesting that low dose Rut supplementation may slightly restore the ability to produce natural antibody IgM in vivo (Fig. 5(D)). Unfortunately, we found that serum IgG levels in the RM group and IgA levels in both RL and RM groups slightly decreased ($p > 0.05$) compared to those in the DC group, respectively (Fig. 5(A) and 5(B)). In comparison with (IgA + IgM)/IgG and IgE/IgG antibody levels ratio, there were not statistically significant ($p > 0.05$) among groups (Fig. 5(E)). Our results suggest that low dose and long term Rut supplementation may enhance the immunity but avoid the adverse side effect in the TRAMP-C1 tumor-bearing mice.

3.6. Rut administration effects on peripheral blood T and B lymphocytes subpopulations in allogeneic TRAMP-C1 prostate cancer mice

To measure the changes in blood T and B lymphocytes in the TRAMP-C1 tumor-bearing mice, the percentage of $CD3^+$ (all T cells), $CD19^+$ (all B cells), $CD4^+$ (helper T cells) and $CD8^+$ (cytotoxic T cells) in peripheral blood were respectively measured using flow cytometry (Fig. S2). The results demonstrated that Rut administration slightly ($p > 0.05$) decreased the percentage of blood $CD3^+$ T cells, but obviously increased the percentage of $CD19^+$ B cells compared to those in the DC group (Fig. 6). TRAMP-C1 tumor-bearing mice (DC group) had significantly ($p < 0.05$) lower $CD19^+$ B cells compared to that in the VC group. Importantly, Rut administration and paclitaxel i.p. (PC group) markedly reversed the percentage of $CD19^+$ B cells in the blood of TRAMP-C1 tumor-bearing mice. Further analyses on $CD3^+$ T cell subpopulations showed that TRAMP-C1 tumor-bearing mice (DC group) had markedly lower $CD4^+$ and $CD8^+$ cells compared to those in the VC group. Importantly, treatments with Rut and paclitaxel i.p. (PC group) slightly ($p > 0.05$) increased the percentage of both $CD4^+$ and $CD8^+$ T lymphocytes. Overall, our results suggest that Rut administration plays a vital role in prostate cancer cell growth inhibition in allogeneic TRAMP-C1 prostate cancer mice via regulating the $CD4^+$, $CD8^+$ and $CD19^+$ lymphocyte subset ratios (Fig. 6).

3.7. Associations between Th1/Th2 cytokine secretion levels in primary splenocyte cultures as well as serum non-specific antibody titers and tumor weights in allogeneic TRAMP-C1 prostate cancer mice treated with Rut in vivo

The relationships between primary splenocyte secretion levels, as well as serum non-specific antibody titers and tumor weights in each individual corresponding Rut-fed TRAMP-C1 prostate cancer mouse

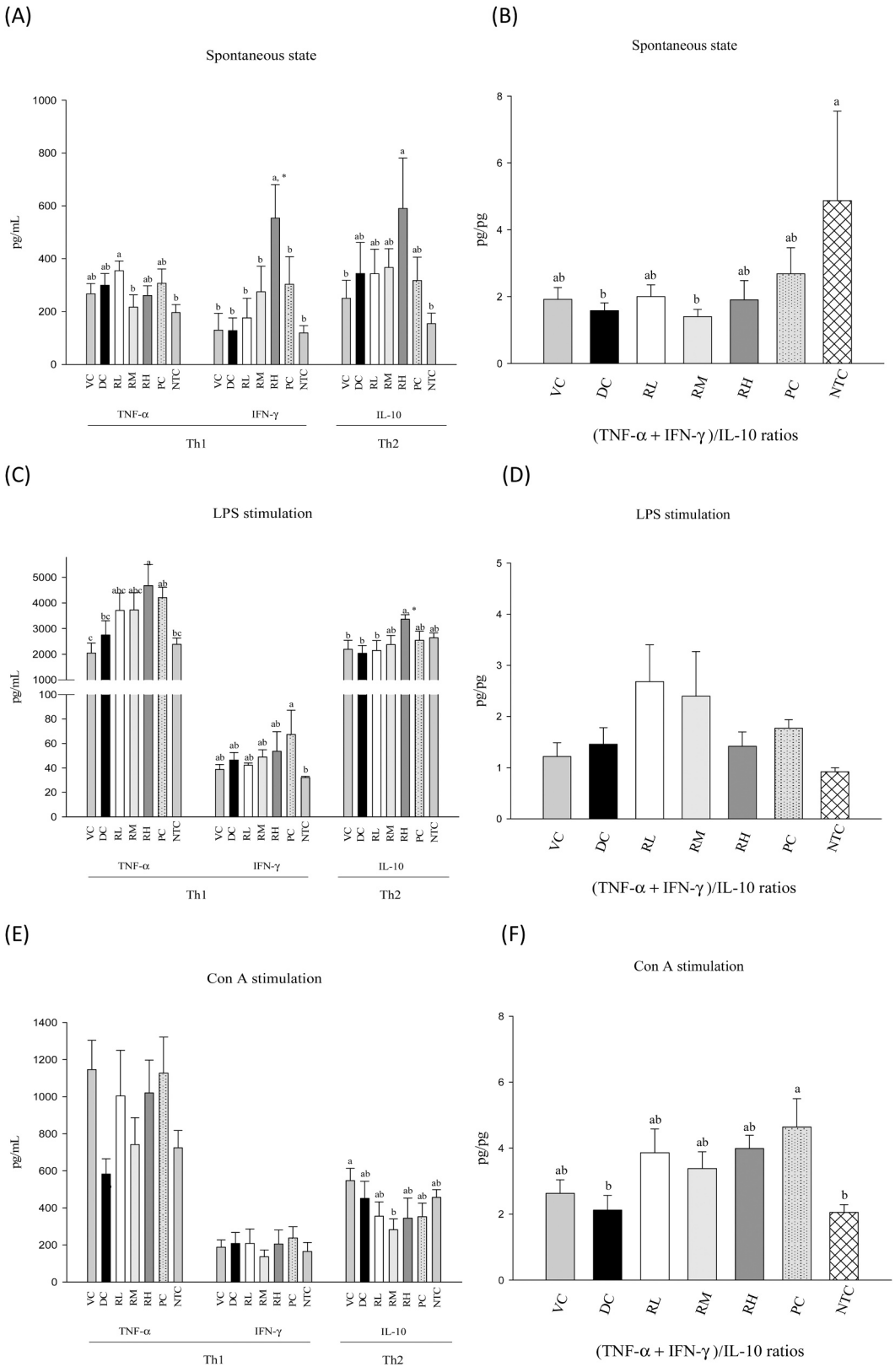

Fig. 3. Rutaecarpine administration effects with different doses on Th1 and Th2 cytokine secretions by splenocytes of male C57BL/6J mice subcutaneously loaded with TRAMP-C1 cells for 39 days. Values are means ± SEM ($n = 6–9$). Bars in same plot within the same cytokine item not sharing a common small letter (a, b, c) are significantly different ($p < 0.05$) from each other analyzed by one-way ANOVA, followed by Duncan's multiple range test. *, Significant differences from DC group analyzed with one-way ANOVA, followed by Dunnett's post hoc test. The original cell density was 5×10^6 cells/mL. The limit of detection (LOD) of cytokine ELISA kits used in this study was <15.6 pg/mL. LPS, lipopolysaccharide at 2.5 μg/mL. Con A, concanavalin A at 2.5 μg/mL. NTC, non-treatment control; VC, vehicle control; DC, dietary control; PC, paclitaxel treatment i.p., a positive control; RL, low dose rutaecarpine; RM, medium dose rutaecarpine; RH, high dose rutaecarpine.

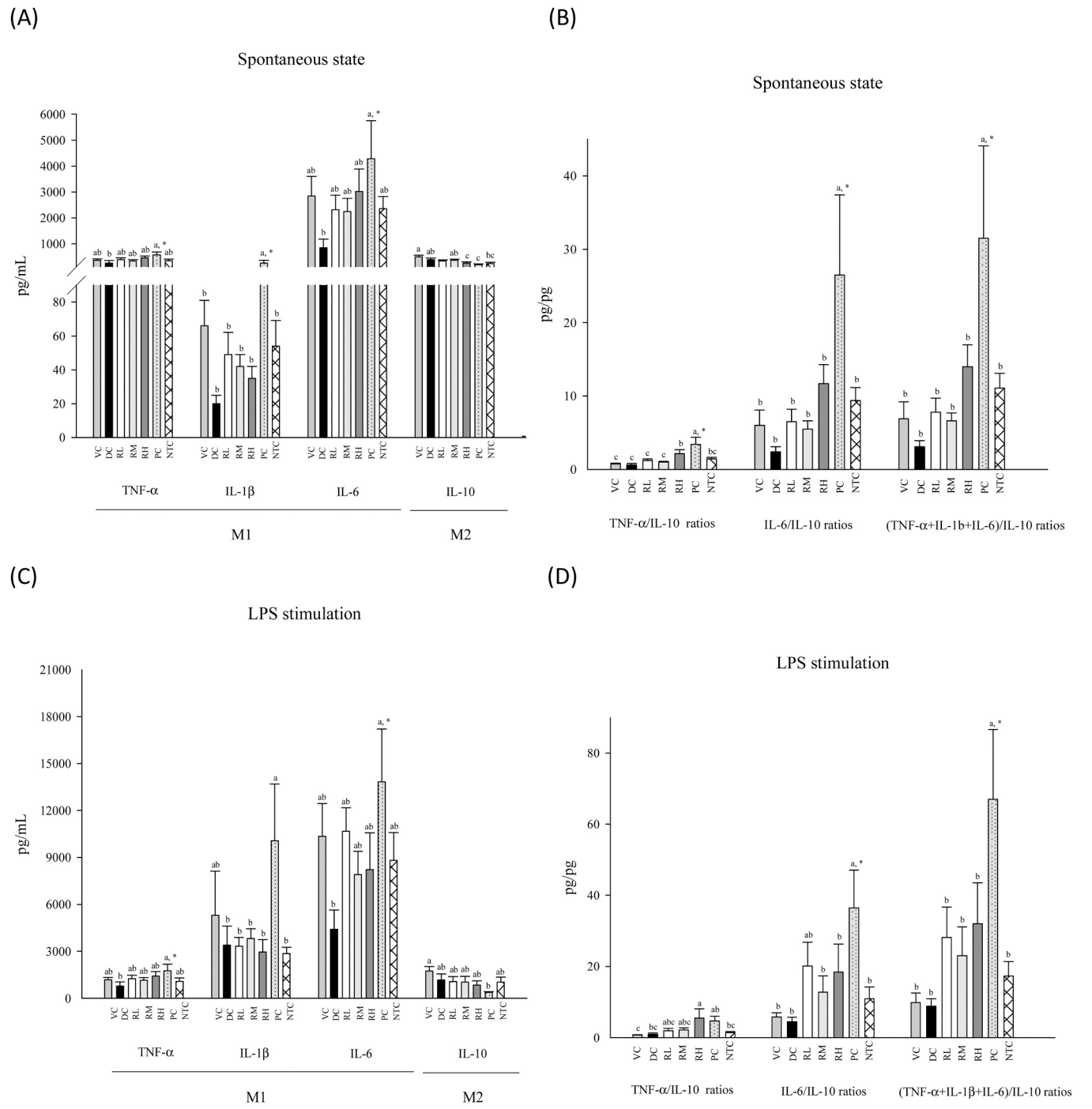

Fig. 4. Rutaecarpine administration effects with different doses on M1 and M2 cytokine secretions by peritoneal cells of male C57BL/6J mice subcutaneously loaded with TRAMP-C1 cells for 39 days. Values are means ± SEM ($n = 6–9$). Bars in the same plot within the same cytokine item not sharing a common small letter (a, b, c) are significantly different ($p < 0.05$) from each other analyzed by one-way ANOVA, followed by Duncan's multiple range test. * , Significant differences from DC group analyzed with one-way ANOVA, followed by Dunnett's post hoc test. The original cell density was 1×10^6 cells/mL. The limit of detection (LOD) of cytokine ELISA kits used in this study was <15.6 ng/mL. LPS, lipopolysaccharide at 2.5 μg/mL. NTC, non-treatment control; VC, vehicle control; DC, dietary control; PC, paclitaxel treatment i.p., a positive control; RL, low dose rutaecarpine; RM, medium dose rutaecarpine; RH, high dose rutaecarpine.

were analyzed using the Pearson product-moment correlation coefficient (r) (Fig. 7). In the spontaneous state, TNF-α cytokine secretions by splenocytes were positively correlated with tumor weights ($r = 0.407$, $^{**}p = 0.003$) (Fig. 7(A)). TNF-α is a potent cancer cachexia factor that can be inhibited by anti-inflammatory cytokine IL-10. Our results evidenced that cancer cachexia may enhance tumor weights in the experimental mice. Moreover, there was a negative correlation between serum IgG levels and tumor weights ($r = -0.356$, $^{*}p = 0.011$) (Fig. 7 (B)). IgG is a Th1-type antibody. Our results evidenced that increased Th1-polarized immune balance may decrease prostate tumor weights in vivo.

4. Discussion

Prostate cancer with a high incidence and mortality is the most common cause of male cancer-related deaths worldwide [36]. To date,

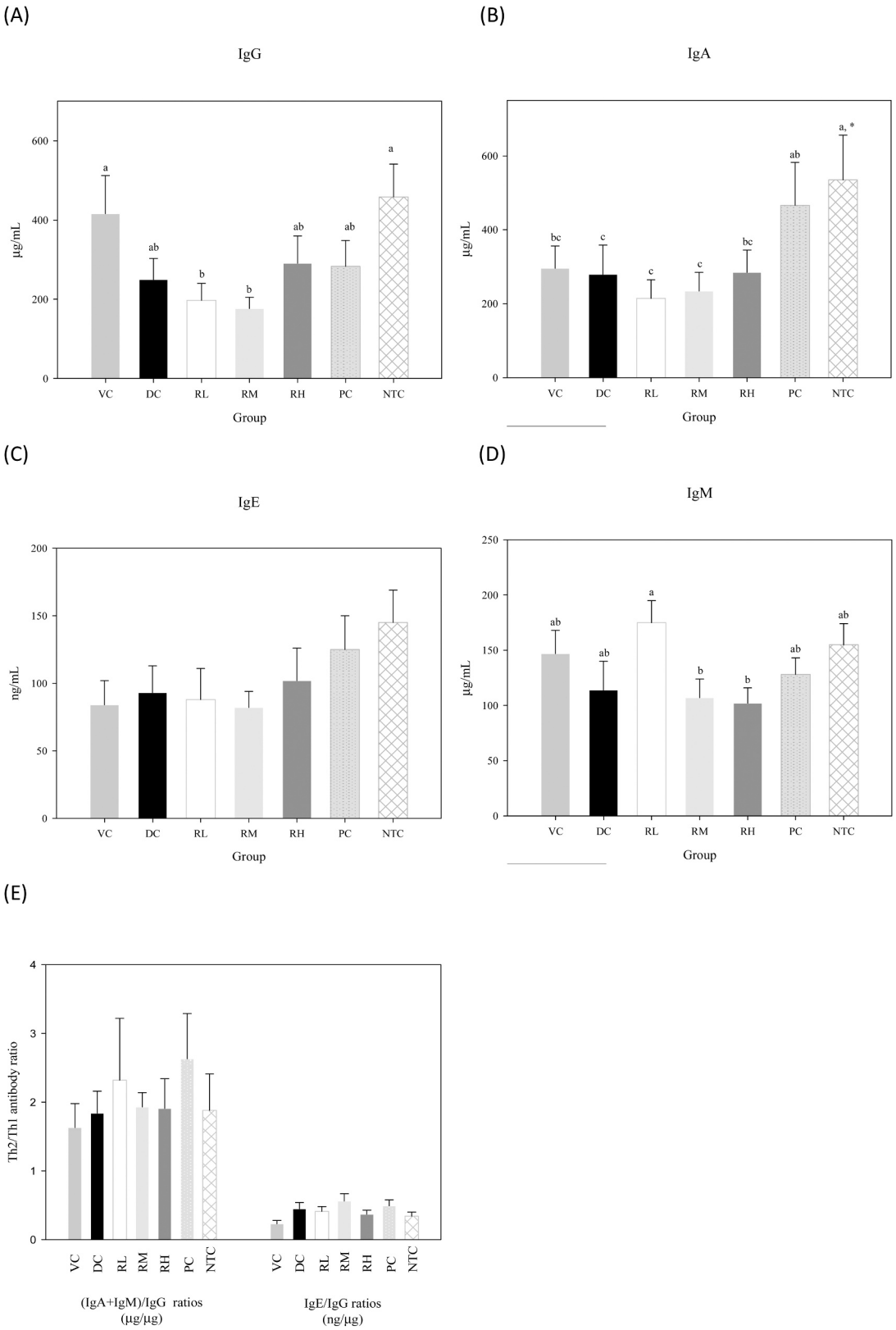

Fig. 5. Rutaecarpine administration effects with different doses on serum non-specific antibody IgA, IgE, IgG and IgM titers of male C57BL/6J mice subcutaneously loaded with TRAMP-C1 cells for 39 days. Values are means ± SEM ($n = 7–9$). Bars in same plot within the same antibody item not sharing a common small letter (a, b, c) are significantly different ($p < 0.05$) from each other analyzed by one-way ANOVA, followed by Duncan's multiple range test. *, Significant differences from DC group analyzed with one-way ANOVA, followed by Dunnett's post hoc test. VC, vehicle control; DC, dietary control; RL, low dose rutaecarpine; RM, medium dose rutaecarpine; RH, high dose rutaecarpine; PC, paclitaxel treatment i.p., a positive control; NTC, non-treatment control. To determine non-specific antibody titers, each collected serum was diluted to 1:10 for IgE, 1:2500 for IgM and IgA, and 1:10000 for IgG, respectively.

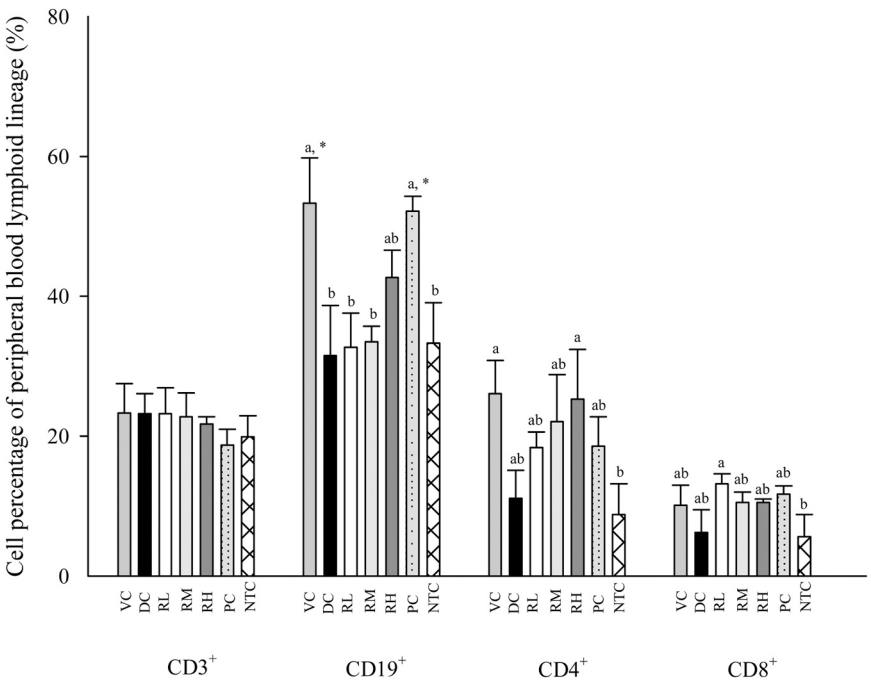

Fig. 6. Rutaecarpine administration effects with different doses on the peripheral blood cell proportion of lymphoid lineage in male C57BL/6J mice subcutaneously loaded with TRAMP-C1 cells for 39 days. Values are means ± SEM ($n = 5$). Bars within same cell type item not sharing a common small letter (a, b) are significantly different ($p < 0.05$) from each other analyzed by one-way ANOVA, followed by Duncan's multiple range test. * , Significant differences from DC group analyzed with one-way ANOVA, followed by Dunnett's post hoc test. VC, vehicle control, DC, dietary control; RL, low dose rutaecarpine; RM, medium dose rutaecarpine; RH, high dose rutaecarpine; PC, paclitaxel, a positive control; NTC, non-treatment control.

some anticancer drugs have been used for killing tumor cells, but they may cause damage to the human body and even further suppress immune function. In general, spontaneous cytokine secretions by primary splenocytes and peritoneal macrophages are much lower compared to those under LPS (a B-cell mitogen and an endotoxin) or Con A (a T-cell mitogen) stimulation. To augment the immune response (e.g., cytokine secretions) in vitro for comparison, LPS (a B-cell mitogen) and Con A (a T-cell mitogen) were selected to treat splenocytes (Fig. 3); LPS (an endotoxin) was selected to treat peritoneal macrophages (Fig. 4). As predicated, LPS (a B-cell mitogen and an endotoxin) and Con A (a T-cell mitogen) enhanced different cytokine secretions by immune cells among groups, respectively (Figs. 3 and 4). In the present study, we found that Rut administration demonstrated an anti-tumor effect (Table 1, Fig. 2), possibly through modulating Th1/Th2 (Fig. 3) and M1/M2 cytokine secretions (Fig. 4) in the cancer microenvironment and changing peripheral blood T and B lymphocytes subpopulations in allogeneic TRAMP-C1 prostate cancer mice (Fig. 6). The production of T lymphocytes with anti-cancer activity is a prerequisite for immunotherapy [14,15]. Consistent with our results, this study suggests that Rut tube feeding for 39 days can reduce the size of tumors, via regulating the immune response toward Th1- and M1-polarized immune balance (Fig. 3 and Fig. 4), increasing T cells or activating B cells (Fig. S2) and macrophages. Some tumor-bearing hosts express M2 type macrophages which suppress immunity to promote tissue repair [37] but accelerate tumor progression that is associated with poor prognosis [38]. Recent studies have pointed out that macrophages may instruct T cells differentiation tendency [12]. We speculate that cytokines secretion by Th1/Th2 cells in the tumor microenvironment may affect macrophage polarization and subsequent prostate cancer progression. In the present study, Rut administration regulated the differentiation tendency of splenocytes and macrophages toward Th1- or M1-polarized cell type to reduce the prostate tumor volume and weight. The results of this study provide direct evidence for treating non-hormonal dependent prostate cancers using Rut administration by gavage in an immunotherapy manner.

The immune cells may act mutually with each other with a synergistic effect, and thus result in anti-prostate cancer effect in vivo. In cancer patients, they often suffer anorexia (appetite loss), sarcopenia, asthenia, and systemic inflammation, etc.; such results are directly related to cancer cachexia [39]. Among cytokines, TNF-α was originally thought to be involved in the development of cachexia. The longer the cancer cachexia duration the greater the possibility for lipid and glucose metabolism. Undoubtedly, this cancer cachexia result may be detrimental to the host [40]. We found that TNF-α is positively correlated with tumor weight in the experiment mice, reflecting the cachexic state in tumor-bearing mice in vivo (Fig. 7(A)). Furthermore, a negative correlation between serum IgG levels and tumor weights ($r = -0.356$, $^*p = 0.011$) was found (Fig. 7(B)), further suggesting that Th1-inclination may be beneficial to inhibit prostate cancer cell growth. We evidenced that Rut tube feeding for 39 days in the mouse model subcutaneously loaded with TRAMP-C1 cells could change the tumor microenvironment to facilitate tumor inhibition.

Traditional herbal medicines with low toxicity are routinely used for anti-tumor treatment and have become a research focus [41,42]. In the present study, Rut administration did not significantly influence the spleen and thymus compared with the DC group, indicating that Rut has little toxicity on immune organs (Table S2). To avoid the possible toxicity of high dose Rut supplementation to prostate cancer patients, the maximum dose of 70 mg Rut/kg b.w/day (high dose, RH, 1.4 mg/20 g mouse/day) for mice was given. This is equal to 543 mg/70 kg b.w./day (= 1.4 mg/20 g mouse/day × 387.9) for humans according to the body surface area ratio between 70 kg human and 20 g mouse [43,44]. Many herbs have been used alone or as a compound prescription which is combined with conventional radiotherapy, chemotherapy, or surgical removal of tumors, such as Zuo-Jin-Wan composed of *Coptis Chinensis* and *Euodia ruticarpa* [45]. The *Euodia ruticarpa* ethanol extract has been found to inhibit human cervical cancer HeLa cell growth via activating AMP-activated protein kinase, increasing caspase-3 and − 9 activities, and further inducing apoptosis [46]. The 70% *Euodia ruticarpa* ethanol extract plays a role in benign prostatic hyperplasia-1 (BPH-1) inhibition with its 5 alpha-reductase inhibitory and apoptotic effects [47]. The alkaloid evodiamine in *Euodia ruticarpa* ethanol extract induces apoptosis through NK and PERK activation in human ovarian cancer cells [48]. Limonin (a compound in *Euodia ruticarpa*) activates the p53 signaling pathway, reduces the viabilities of SKOV-3, A2780, and MUG-S cells, especially Cis^R SKOV-3 cell line and reverses the drug resistance [49]. Zuo-Jin-Wan (ZJW), a two-herb formula containing *Coptis chinensis* and *Euodia ruticarpa*, was found to suppress cancer cell growth through

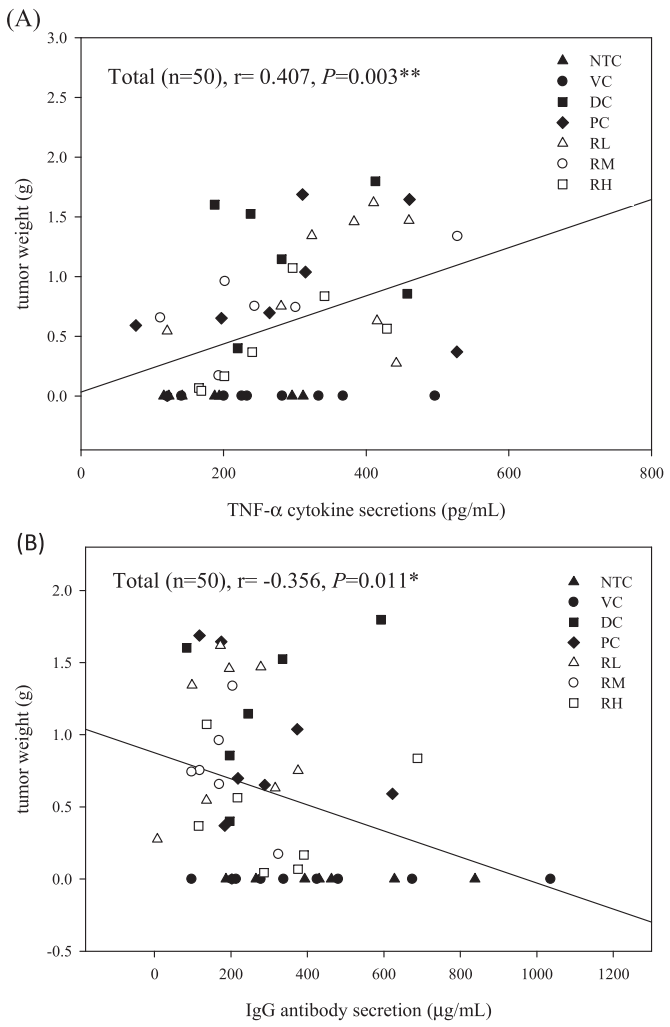

Fig. 7. The relationship between tumor weights and TNF-α secretions by splenocytes **(A)** and serum IgG antibody levels **(B)** from male C57BL/6J mice subcutaneously loaded with TRAMP-C1 cells treated with rutaecarpine by gavage for 39 days. The correlation was expressed by Pearson product-moment correlation coefficient (r). *, $p < 0.05$; **, $p < 0.01$.

c-myc signaling pathways in orthotopic HepG2 xenograft-bearing mice [50]. *Euodia ruticarpa* steam distilled essential oils have been found to possess anti-inflammatory effects and anti-cancer potential [28]. Rut has been subjected to analyze its pharmacokinetics (PK) with qualitative and quantitative determination of the metabolites in the urine of male Sprague-Dawley (SD) rats detected by liquid chromatography–electrospray ionization–mass spectrometry (LC–ESI–MS) after oral administration of Evodiae fructus and Zuo-Jin-Wan (ZJW) preparation. Three metabolites, hydroxydehydroevodiamine sulfate, dehydroevodiamine glucoronide, and hydroxyevodiamine glucuronide, were detected during 48 h. More metabolites within 0–24 h were eliminated than those within 24–48 h [51]. After oral administration of the same concentration of 40 mg Rut/kg b.w. in SD rats for 18 days, the C_{max} value ($\geq$ 22.8 $\pm$ 4.4 ng/mL) of the Rut purity group was higher than that in the crude drug (2.4 $\pm$ 0.3 ng/mL), indicating that the herbal extract can increase the bioavailability of Rut in SD rats [52,53]. Moreover, the values of $T_{1/2}$, volume and AUC0-t in the plasma of Rut by intravenously administrated to the rats were 29.29 min, 655.15 mL/kg, and 32.93 μg min/mL, respectively [54]. Rut's pharmacokinetic values may be helpful to its use in biomedicine and pharmacotherapy. Moreover, after oral supplementation to SD rats, 16 metabolites and Rut drug itself in plasma, including 3 phase I, 12 phase II metabolites and Rut, were detected using UHPLC-LTQ-Orbitrap MS [55]. To date, the main pharmacological targets of Rut still focus on cardiovascular and circulatory systems and it can be metabolized by human cytochrome P450 enzymes [56,57]. However, Rut has been shown a selective inhibitor to inhibit the oxidation catalyzed by CYP1A [58]. In our preliminary in vitro experiments, macrophages conditioned media inhibited the growth of TRAMP-C1 cells, implying that immune cells may directly affect the growth of TRAMP-C1 cells. Undoubtedly, Rut is a direct stimulant to immune cells. However, we assume that the effect of Rut on the growth of TRAMP-C1 cells in vivo may be through both direct action and indirect immunotherapy [59]. In the present study we evidenced that Rut, which is a plant alkaloid abundant in *Euodia ruticarpa,* may be used for treating prostate cancer in vivo. Based on the present study, Rut may be applied to treat prostate cancer for humans via both direct action and immunotherapy in the future.

This study adopted a subcutaneous allograft model to explore the effect of Rut on prostate cancer, which is a short cycle and simple operation animal model. To date, it is commonly used prostate cancer animal model because it maintains most of the biological characteristics of the primary tumor, high tumor formation rate, and short experimental period. However, the tumor in this animal model does not metastasize, so it is generally used in an evaluation research for cancer growth and proliferation and anti-tumor efficacy. Rut is a quinazolinocarboline alkaloid identified from *Euodia ruticarpa*. It has been proven that Rut and its analogs have a variety of anti-tumor activities, including human lung adenocarcinoma (A549), human colon cancer (HT-29), leukemia (CCRF-CEM), non-small cell lung cancer (A549/ATCC and NCI-11460), kidney cancer (786-0), ovarian cancer (OVCAR-4), and breast cancer (HS-578T). Maybe, Rut could be developed a universal anti-cancer drug for most types of cancers in the future. However, more research data should be accumulated.

5. Conclusions

Rutaecarpine (Rut) is a plant alkaloid rich in *Euodia ruticarpa* used as a Chinese herb medicine for treating various cancers. To clarify the Rut administration effect on prostate cancer, an allogeneic TRAMP-C1 prostate cancer mouse animal model was established for evaluating Rut's anti-prostate cancer effects. The evidence showed that Rut administration significantly suppressed prostate cancer volume and weight in the orthotopic TRAMP-C1 tumor-bearing mice. Little toxicity was found in the immune organs in vivo. Rut administration regulated the differentiation tendency of splenocytes and macrophages toward Th1- and M1-polarized cell types in vivo, respectively. Treatments with Rut by gavage for 39 days enhanced the immunity via regulating and increasing the blood $CD4^+$, $CD8^+$ and $CD19^+$ lymphocyte subset ratios in the allogeneic TRAMP-C1 prostate cancer mice. Analyses of correlations evidenced that a TNF-α cytokine, which is a cancer cachexia potent factor, may increase tumor weights in the experimental mice. However, there was a negative correlation between serum IgG (a Th1-type antibody) levels and tumor weights, suggesting that increased Th1 immune balance may decrease TRAMP-C1 prostate cancer weights in vivo. The present study is the first report to evidence Rut's anti-prostate cancer effects in vivo. Rut may be further applied to treat prostate cancer in humans in the future.

Funding

Ministry of Science and Technology (Taiwan) kindly supported research grants MOST 104-2320-B-005-006-MY3 and MOST 107-2320-B-005-010-MY3 for this study.

CRediT authorship contribution statement

Jin-Yuarn Lin: Data curation, Formal analysis, Investigation, Writing - original draft. **Tzu-He Yeh:** Conceptualization, Methodology, Validation, Writing - review & editing, Funding acquisition.

Declaration of Competing Interest

The authors declare that they have no known competing financial interests or personal relationships that could have appeared to influence the work reported in this paper.

Appendix A. Supporting information

Supplementary data associated with this article can be found in the online version at doi:10.1016/j.biopha.2021.111648.

References

[1] R.L. Siegel, K.D. Miller, H.E. Fuchs, A. Jemal, Cancer statistics, CA Cancer J. Clin. 71 (2021) 7–33, https://doi.org/10.3322/caac.21654.

[2] R.V. Gopalkrishnan, D.C. Kang, P.B. Fisher, Molecular markers and determinants of prostate cancer metastasis, J. Cell Physiol. 189 (2001) 245–256, https://doi.org/10.1002/jcp.10023.

[3] Z. Long, B. Chen, Q. Liu, J. Zhao, Z. Yang, X. Dong, L. Xia, S. Huang, X. Hu, B. Song, The reverse-mode NCX1 activity inhibitor KB-R7943 promotes prostate cancer cell death by activating the JNK pathway and blocking autophagic flux, Oncotarget 7 (2016) 42059–42070, https://doi.org/10.18632/oncotarget.9806.

[4] S. Maeda, M. Omata, Inflammation and cancer: role of nuclear factor-kappaB activation, Cancer Sci. 99 (2008) 836–842, https://doi.org/10.1111/j.1349-7006.2008.00763.x.

[5] A. Mantovani, F. Marchesi, A. Malesci, L. Laghi, P. Allavena, Tumour-associated macrophages as treatment targets in oncology, Nat. Rev. Clin. Oncol. 14 (2017) 399–416, https://doi.org/10.1038/nrclinonc.2016.217.

[6] B.Z. Qian, J.W. Pollard, Macrophage diversity enhances tumor progression and metastasis, Cell 141 (2010) 38–51, https://doi.org/10.1016/j.cell.2010.03.014.

[7] H.R. Cha, J.H. Lee, S. Ponnazhagan, Revisiting immunotherapy: a focus on prostate cancer, Cancer Res. 80 (2020) 1615–1623, https://doi.org/10.1158/0008-5472.CAN -19-2948.

[8] S. Gordon, A. Pluddemann, F. Martinez Estrada, Macrophage heterogeneity in tissues: phenotypic diversity and functions, Immunol. Rev. 262 (2014) 36–55, https://doi.org/10.1111/imr.12223.

[9] R. Noy, J.W. Pollard, Tumor-associated macrophages: from mechanisms to therapy, Immunity 41 (2014) 49–61, https://doi.org/10.1016/j.immuni.2014.06.010.

[10] F. Raggi, S. Pelassa, D. Pierobon, F. Penco, M. Gattorno, F. Novelli, A. Eva, L. Varesio, M. Giovarelli, M.C. Bosco, Regulation of human macrophage M1–M2 polarization balance by hypoxia and the triggering receptor expressed on myeloid cells-1, Front. Immunol. 8 (2017) 1097, https://doi.org/10.3389/fimmu.2017.01097.

[11] J.P. Edwards, X. Zhang, K.A. Frauwirth, D.M. Mosser, Biochemical and functional characterization of three activated macrophage populations, J. Leukoc. Biol. 80 (2006) 1298–1307, https://doi.org/10.1189/jlb.0406249.

[12] B. Bartlett, H.P. Ludewick, A. Misra, S. Lee, G. Dwivedi, Macrophages and T cells in atherosclerosis: a translational perspective, Am. J. Physiol. Heart Circ. Physiol. 317 (2019) H375–H386, https://doi.org/10.1152/ajpheart.00206.2019.

[13] F.O. Martinez, S. Gordon, The M1 and M2 paradigm of macrophage activation: time for reassessment, F1000Prime Rep. 6 (2014) 13, https://doi.org/10.12703/P6-13.

[14] D.D. Mitri, M. Mirenda, J. Vasilevska, A. Calcinotto, N. Delaleu, A. Revandkar, V. Gil, G. Boysen, M. Losa, S. Mosole, Re-education of tumor-associated macrophages by CXCR2 blockade drives senescence and tumor inhibition in advanced prostate cancer, Cell Rep. 28 (2019) 2156–2168, https://doi.org/10.1016/j.celrep.2019.07.068.

[15] Q. Meng, Z. Liu, E. Rangelova, T. Poiret, A. Ambati, L. Rane, S. Xie, C. Verbeke, E. Dodoo, M.D. Chiaro, M. Löhr, R. Segersvärd, M.J. Maeurer, Expansion of tumor-reactive T cells from patients with pancreatic cancer, J. Immunother. 39 (2016) 81–89, https://doi.org/10.1097/CJI.0000000000000111.

[16] P. Hradicka, J. Beal, M. Kassayova, A. Foey, V. Demeckova, A novel lactic acid bacteria mixture: macrophage-targeted prophylactic intervention in colorectal cancer management, Microorganisms 8 (2020) 387, https://doi.org/10.3390/microorganisms8030387.

[17] X. Xiang, N. Cao, F. Chen, L. Qian, Y. Wang, Y. Huang, Y. Tian, D. Xu, W. Li, Polysaccharide of Atractylodes Macrocephala Koidz (PAMK) alleviates cyclophosphamide-induced immunosuppression in mice by upregulating CD28/IP3R/PLCγ-1/AP-1/NFAT signal pathway, Front. Pharmacol. 11 (2020), 529657, https://doi.org/10.3389/fphar.2020.529657.

[18] Y. Zhang, Y. Zhang, W. Gao, R. Zhou, F. Liu, T.B. Ng, A novel antitumor protein from the mushroom Pholiota nameko induces apoptosis of human breast adenocarcinoma MCF-7 cells in vivo and modulates cytokine secretion in mice bearing MCF-7 xenografts, Int. J. Biol. Macromol. 164 (2020) 3171–3178, https://doi.org/10.1016/j.ijbiomac.2020.08.187.

[19] K.M. Tian, J.J. Li, S.W. Xu, Rutaecarpine: a promising cardiovascular protective alkaloid from Evodia rutaecarpa (Wu Zhu Yu), Pharmacol. Res. 141 (2019) 541–550, https://doi.org/10.1016/j.phrs.2018.12.019.

[20] S. Xu, J. Peng, Y. Li, L. He, F. Chen, J. Zhang, J. Ding, Pharmacokinetic comparisons of rutaecarpine and evodiamine after oral administration of Wu-Chu-Yu extracts with different purities to rats, J. Ethnopharmacol. 139 (2012) 395–400, https://doi.org/10.1016/j.jep.2011.11.023.

[21] Z. Zhao, X. He, W. Han, X. Chen, P. Liu, X. Zhao, X. Wang, L. Zhang, S. Wu, X. Zheng, Genus Tetradium L.: a comprehensive review on traditional uses, phytochemistry, and pharmacological activities, J. Ethnopharmacol. 231 (2019) 337–354, https://doi.org/10.1016/j.jep.2018.11.035.

[22] J.Q. Cao, S.S. Guo, Y. Wang, X. Pang, Z.F. Geng, S.S. Du, Contact toxicity and repellency of the essential oils of Evodia lenticellata Huang and Evodia rutaecarpa (Juss.) Benth. Leaves against three stored product Insects, J. Oleo Sci. 67 (2018) 1027–1034, https://doi.org/10.5650/jos.ess17251.

[23] J. Deng, J. Qin, Y. Cai, X. Zhong, X. Zhang, S. Yu, Rutaecarpine suppresses proliferation and promotes apoptosis of human pulmonary artery smooth muscle cells in hypoxia possibly through HIF-1alpha-dependent pathways, J. Cardiovasc. Pharm. 71 (2018) 293–302, https://doi.org/10.1097/FJC.0000000000000571.

[24] L. Ji, M. Wu, Z. Li, Rutacecarpine inhibits angiogenesis by targeting the VEGFR2 and VEGFR2-mediated Akt/mTOR/p70s6k signaling pathway, Molecules 23 (2018) 2047, https://doi.org/10.3390/molecules23082047.

[25] Z. Li, M. Yang, Y. Peng, M. Gao, B. Yang, Rutaecarpine ameliorated sepsis-induced peritoneal resident macrophages apoptosis and inflammation responses, Life Sci. 228 (2019) 11–20, https://doi.org/10.1016/j.lfs.2019.01.038.

[26] J. Ma, L. Chen, J. Fan, W. Cao, G. Zeng, Y. Wang, Y. Li, Y. Zhou, X. Deng, Dual-targeting rutaecarpine-NO donor hybrids as novel anti-hypertensive agents by promoting release of CGRP, Eur. J. Med. Chem. 168 (2019) 146–153, https://doi.org/10.1016/j.ejmech.2019.02.037.

[27] X. Pan, M. Wang, Y. Wu, X. Lu, Y. Shang, Y. Xu, Y. Zhai, J. Li, Z. Li, M. Gong, Identification of active ingredients in Wuzhuyu decoction improving migraine in mice by spectral efficiency association, Mol. Med. Rep. 12 (2015) 1524–1534, https://doi.org/10.3892/mmr.2015.3506.

[28] T.H. Yeh, J.Y. Lin, Acorus gramineusand and Euodia ruticarpa steam distilled essential oils exert anti-inflammatory effects through decreasing Th1/Th2 and pro-/anti-inflammatory cytokine secretion ratios In Vitro, Biomolecules 10 (2020) 338, https://doi.org/10.3390/biom10020338.

[29] S.Y. Zeng, L. Yang, H.Q. Lu, Q.J. Yan, L. Gao, X.P. Qin, Rutaecarpine prevents hypertensive cardiac hypertrophy involving the inhibition of Nox4-ROS-ADAM17 pathway, J. Cell Mol. Med. 23 (2019) 4196–4207, https://doi.org/10.1111/jcmm.14308.

[30] M. Masi, S.V. slambrouck, S. Gunawardana, M.J. van Rensburg, P.C. James, J. G. Mochel, P.S. Heliso, A.S. Albalawi, A. Cimmino, W.A.L. van Otterlo, A. Kornienko, I.R. Green, A. Evidente, Alkaloids isolated from Haemanthus humilis Jacq., an indigenous south african amaryllidaceae: anticancer activity of coccinine and montanine, S. Afr. J. Bot. 126 (2019) 277–281, https://doi.org/10.1016/j.sajb.2019.01.036.

[31] H. Mekky, J. Al-Sabahi, M.F.M. Abdel-Kreem, Potentiating biosynthesis of the anticancer alkaloids vincristine and vinblastine in callus cultures of Catharanthus roseus, S. Afr. J. Bot. 114 (2018) 29–31, https://doi.org/10.1016/j.sajb.2017.10.008.

[32] S. Vergura, E. Santoro, M. Masi, A. Evidente, P. Scafato, S. Superchi, G. Mazzeo, G. Longhi, S. Abbate, Absolute configuration assignment to anticancer Amaryllidaceae alkaloid jonquailine, Fitoterapia 129 (2018) 78–84, https://doi.org/10.1016/j.fitote.2018.06.013.

[33] Y.N. Liao, Y. Liu, X.H. Xia, Z.L. Shao, C.Y. Huang, J.C. He, L.L. Jiang, D.L. Tang, J. B. Liu, H.B. Huang, Targeting GRP78-dependent AR-V7 protein degradation overcomes castration-resistance in prostate cancer therapy, Theranostics 10 (2020) 3366–3381, https://doi.org/10.7150/thno.41849.

[34] American Institute of Nutrition Ad Hoc C, Report of the american institute of nutrition ad hoc committee on standards for nutritional studies, J. Nutr. 107, pp. 1340–1348 (1977). https://doi.org/10.1093/jn/107.7.1340.

[35] C.J. Liu, J.Y. Lin, Anti-inflammatory effects of phenolic extracts from strawberry and mulberry fruits on cytokine secretion profiles using mouse primary splenocytes and peritoneal macrophages, Int. Immunopharmacol. 16 (2013) 165–170, https://doi.org/10.1016/j.intimp.2013.03.032.

[36] B.T. Rekoske, D.G. McNeel, Immunotherapy for prostate cancer: false promises or true hope ? Cancer 122 (2016) 3598–3607, https://doi.org/10.1002/cncr.30250.

[37] C. Godson, M. Perretti, Novel pathways in the yin-yang of immunomodulation, Curr. Opin. Pharmacol. 13 (2013) 543–546, https://doi.org/10.1016/j.coph.2013.06.010.

[38] I. Rhee, Diverse macrophages polarization in tumor microenvironment, Arch. Pharm. Res. 39 (2016) 1588–1596, https://doi.org/10.1007/s12272-016-0820-y.

[39] D.S.S. Peixoto, J.M.O. Santos, E.S.M. Costa, D.C.R. Gil, R. Medeiros, Cancer cachexia and its pathophysiology: links with sarcopenia, anorexia and asthenia, J. Cachex. Sarcopenia Muscle 11 (2020) 619–635, https://doi.org/10.1002/jcsm.12528.

[40] C. Popa, M.G. Netea, P.L.C.M. Van Riel, J.W.M. Van Der Meer, A.F.H. Stalenhoef, The role of TNF-α in chronic inflammatory conditions, intermediary metabolism, and cardiovascular risk, J. Lipid Res. 48 (2007) 751–762, https://doi.org/10.1194/jlr.R600021- JLR200.

[41] K.C. Kim, J.H. Yook, J. Eisenbraun, B.S. Kim, R. Huber, Quality of life, immunomodulation and safety of adjuvant mistletoe treatment in patients with gastric carcinoma - a randomized, controlled pilot study, BMC Complement. Altern. Med. 12 (2012) 172, https://doi.org/10.1186/1472-6882-12-172.

[42] L. Xu, H. Li, Z. Xu, Z. Wang, L. Liu, J. Tian, J. Sun, L. Zhou, Y. Yao, L. Jiao, Multi-center randomized double-blind controlled clinical study of chemotherapy combined with or without traditional chinese medicine on quality of life of postoperative non-small cell lung cancer patients, BMC Complement. Altern. Med. 12 (2012) 1133, https://doi.org/10.1186/1472-6882-12-112.

[43] M.S. Miao. Experimental Animal and Animal Experiment Technique, China Press of Traditional Chinese Medicine,, Beijing, 1997, pp. 143–145.
[44] H.H. Chang, C.S. Chen, J.Y. Lin, High dose Vitamin C supplementation increases the Th1/Th2 cytokine secretion ratio, but decreases eosinophilic infiltration in bronchoalveolar lavage fluid of ovalbumin-sensitized and challenged mice, J. Agric. Food Chem. 57 (2009) 10471–10476, https://doi.org/10.1021/jf902403p.
[45] S. Huang, Z. Zhang, W. Li, F. Kong, P. Yi, J. Huang, D. Mao, W. Peng, S. Zhang, Network pharmacology-based prediction and verification of the active ingredients and potential targets of Zuojinwan for treating colorectal cancer, Drug Des. Devel. Ther. 14 (2020) 2725–2740, https://doi.org/10.2147/DDDT.S250991.
[46] S.Y. Park, C. Park, S.H. Park, S.H. Hong, G.Y. Kim, S.H. Hong, Y.H. Choi, Induction of apoptosis by ethanol extract of Evodia rutaecarpa in HeLa human cervical cancer cells via activation of AMP-activated protein kinase, Biosci. Trends 10 (2016) 467–476, https://doi.org/10.5582/bst.2016.01170.
[47] S.A. Kaplan, Re: Ethanol extract of Evodia rutaecarpa attenuates cell growth through caspase-dependent apoptosis in benign prostatic hyperplasia-1 cells, J. Urol. 201 (2019) 1030, https://doi.org/01.JU.0000554644.86435.6c.
[48] T.C. Chen, C.C. Chien, M.S. Wu, Y.C. Chen, Evodiamine from Evodia rutaecarpa induces apoptosis via activation of JNK and PERK in human ovarian cancer cells, Phytomedicine 23 (2016) 68–78, https://doi.org/10.1016/j.phymed.2015.12.003.
[49] J.R. Bae, W.H. Park, D.H. Suh, J.H. No, Y.B. Kim, K. Kim, Role of limonin in anticancer effects of Evodia rutaecarpa on ovarian cancer cells, BMC Complement Med. Ther. 20 (2020) 94, https://doi.org/10.1186/s12906-020-02890-y.
[50] S.T. Chou, C.Y. Hsiang, H.Y. Lo, H.F. Huang, M.T. Lai, C.L. Hsieh, S.Y. Chiang, T. Y. Ho, Exploration of anti-cancer effects and mechanisms of Zuo-Jin-Wan and its alkaloid components in vitro and in orthotopic HepG2 xenograft immunocompetent mice, BMC Complement. Altern. Med. 17 (2017) 121, https://doi.org/10.1186/s12906-017-1586-6.
[51] R. Yan, Q. Mu, Y. Wang, Y. Liu, X. Di, Characterization and determination of the alkaloid metabolites of Evodiae fructus in rat urine by liquid chromatography-tandem mass spectrometry detection, Molecules 16 (2011) 5822–5832.
[52] J.S. Ding, R. Gao, D. Li, J. Peng, L.L. Ran, Y.J. Li, Solid dispersion of rutaecarpine improved its antihypertensive effect in spontaneously hypertensive rats, Biopharm. Drug Dispos. 29 (2008) 495–500.
[53] S. Xu, J. Peng, Y. Li, L. He, F. Chen, J. Zhang, J. Ding, Pharmacokinetic comparisons of rutaecarpine and evodiamine after oral administration of Wu-Chu-Yu extracts with different purities to rats, J. Ethnopharmacol. 139 (2012) 395–400.
[54] H.C. Ko, T.H. Tsai, C.J. Chou, S.Y. Hsu, S.Y. Li, C.F. Chen, High-performance liquid chromatographic determination of rutaecarpine in rat plasma: application to a pharmacokinetic study, J. Chromatogr. B 655 (1994) 27–31.
[55] W. Cai, Y. Guan, Y. Zhou, Y. Wang, H. Ji, Z. Liu, Detection and characterization of the metabolites of rutaecarpine in rats based on ultra-high-performance liquid chromatography with linear ion trap-Orbitrap mass spectrometer, Pharm. Biol. 55 (2017) 294–298.
[56] Y.F. Ueng, M.J. Don, W.C. Jan, S.Y. Wang, L.K. Ho, C.F. Chen, Oxidative metabolism of the alkaloid rutaecarpine by human cytochrome P450, Drug Metab. Dispos. 34 (2006) 821–827.
[57] S. Rendic, F.J.D. Carlo, Human cytochrome P450 enzymes: a status report summarizing their reactions, substrates, inducers, and inhibitors, Drug Metab. Rev. 29 (1997) 413–580.
[58] Y.F. Ueng, W.C. Jan, L.C. Lin, T.L. Chen, F.P. Guengerich, C.F. Chen, The alkaloid rutaecarpine is a selective inhibitor of cytochrome P450 1A in mouse and human liver microsomes, Drug Metab. Dispos. 30 (2002) 349–353.
[59] H.C. Lin, J.Y. Lin, Pharmacological effects of guava (Psidium guajava L.) seed polysaccharides: GSF3 inhibits PC-3 prostate cancer cell growth through immunotherapy in vitro, Int. J. Mol. Sci. 22 (2021) 3631, https://doi.org/10.3390/ijms22073631.